J Mater Sci (2007) 42:4291–4297
DOI 10.1007/s10853-006-1232-z

Containerless processing of a lithium disilicate glass

K. S. Ranasinghe · C. S. Ray · D. E. Day · J. R. Rogers · R. W. Hyers · T. Rathz

Received: 18 August 2005 / Accepted: 6 February 2006 / Published online: 28 February 2007

Abstract Glasses of $Li_2O \cdot 2SiO_2$ (LS_2), and LS_2 doped with 0.001 wt% platinum (LS_2 + 0.001 wt% Pt) compositions were melted, cooled and reheated at controlled rates while levitated (containerless) inside an electrostatic levitator (ESL) furnace at the NASA Marshall Space Flight Center. The experiments were conducted in vacuum using spherical, 2.5–3 mm diameter, glass samples. The measured critical cooling rate for glass formation, R_c, for the LS_2 and LS_2 + 0.001 wt% Pt glasses processed at ESL were 14 ± 2 °C/min and 130 ± 5 °C/min, respectively. The values of R_c for the same LS_2 and LS_2 + 0.001 wt% Pt glasses processed in a container were 62 ± 3 °C/min and 162 ± 5 °C/min, respectively. The effective activation energy for crystallization, E, for this LS_2 glass processed without a container at ESL, was higher than that for an identical glass processed in a container. These results suggest that the glass formation tendency for a containerless LS_2 melt is significantly increased compared to an identical melt in contact with a container. The absence of heterogeneous nucleation sites that are inherently present in all melts held in containers is believed to be the reason for the increased glass forming tendency of this containerless melt.

K. S. Ranasinghe (✉)
Department of Physics and Geology, Northern Kentucky University, Nunn Drive, Highland Heights, KY 41099, USA
e-mail: ranasinghk1@nku.edu

C. S. Ray · J. R. Rogers
Marshall Space Flight Center, National Aeronautics and Space Administration, Huntsville, AL 35812, USA

D. E. Day
Graduate Center for Materials Research, University of Missouri-Rolla, Rolla, MO 65409, USA

R. W. Hyers
Department of Mechanical and Industrial Engineering, University of Massachusetts, Amherst, MA 01003, USA

T. Rathz
University of Alabama in Huntsville, Huntsville, AL 35899, USA

Introduction

Containerless processing of high temperature melts has the advantage of eliminating container-induced impurities into the melts, which cannot be avoided in melts in contact with a container. It is known that the presence of foreign particles can enhance the nucleation and crystallization tendency of a glass by the process of heterogeneous nucleation [1–7]. The foreign particles act as nucleating sites/agents on which the nuclei develop and grow.

In glass forming melts, the container-induced impurities often act as potential sites for heterogeneous nucleation/crystallization, thereby, increasing the crystallization tendency or reducing the glass forming tendency of the melt. The compositional region for glass formation of a system can be extended or the glass formation tendency for a melt of a particular composition can be increased if these compositions are melted and solidified in a containerless fashion, thereby, facilitating glass formation for melts that are reluctant to form glass when processed in a container. Containerless processing also provides a unique way

for preparing glasses of ultra-high purity and, hence, of special properties even from melts that are highly reactive to most known container materials.

The glass formation tendency for a melt is generally estimated from its critical cooling rate for glass formation, R_c, which is the slowest rate at which a melt can be cooled without crystallization [8, 9]. A smaller R_c indicates a higher tendency for glass formation or a smaller tendency for crystallization of the melt. Like wise, the effective activation energy, E, for crystallization can also be used as a measure for the tendency for glass formation of a melt [10]. A higher value of E implies a larger tendency for a melt to form glass. The objective of the present work is to determine whether containerless processing improves glass formation of melts by measuring their critical cooling rate, R_c and the effective activation energy, E; and comparing these values with those for the same melts processed in a container. Although, the hypothesis for improving the glass forming ability of a melt by suppressing heterogeneous nucleation through containerless processing seems reasonable, it has not been experimentally demonstrated up to this time for glass forming, inorganic oxide melts.

The electrostatic levitation (ESL) system at the NASA Marshall Space Flight Center (MSFC, Huntsville, AL) [11, 12] was used for the present containerless experiments. In the family of containerless processing facilities, ESL has the capability of levitating a wide range of materials [13–16], including glass forming melts based on inorganic oxides (non-conducting) [17, 18] that are of interest in the present investigation. Melts of $Li_2O \cdot 2SiO_2$ composition (hereafter referred to as LS_2) and LS_2 doped with 0.001 wt% Pt particles as heterogeneous nucleating agent were used. The LS_2 melt was selected primarily for the reason that a glass of this composition is widely used as a model glass for investigating nucleation and crystallization kinetics, and the properties that are of interest in the present investigation are available for this glass [19–25].

The present work at MSFC-ESL was undertaken due to reports [26–29], which suggest that the glass forming tendency for melts processed in low-gravity (space) is increased compared to identical melts processed at 1-g on earth. However, it is not known whether the observed increase in glass formation for the space melts is due to containerless processing, or the effect of low-gravity, or both. Measuring the glass formation or crystallization tendency for a melt under containerless condition at ESL on earth (1-g) and comparing these results with those from the containerless experiments in space (low-g) will help identify and separate the respective roles of containerless processing and low-gravity on the kinetics of melt solidification.

Experiment

Sample preparation

A well mixed batch of 33.3 mol% Li_2CO_3 (purity 99.0%, Alfa Aesar) and 66.7mol% crystalline SiO_2 (purity 99.9%, Alfa Aesar) that produced about 20 g of LS_2 glass was melted in an electric furnace at about 1400 °C for 3h in a platinum/10% rhodium crucible. The melt was stirred three times with an alumina rod at intervals of ~45 min to ensure homogeneity. Glass fibers with a diameter between 0.25–0.50 mm and 500 mm long were drawn from the melt by hand. One end of the glass fiber was melted using a fine tipped propane torch. As the fiber melted and formed a spherical glass bead, a critical weight-to-surface tension value was reached at which the sphere detached from the rest of the fiber. By controlling the length of the fiber in the melted zone, glass spheres of various diameters could be easily prepared. The density of the melt limits the maximum size of the spheres that can be produced by this technique. For the LS_2 glass, spheres with diameters of 3.0 ± 0.5 mm (masses between 20 mg and 30 mg) were found highly suitable for stable levitation in the ESL. LS_2 glass spheres containing 0.001 wt% Pt as heterogeneous nucleating agents were also prepared by the same method and used to investigate the effect of heterogeneous nucleation on the critical cooling rate for glass formation of containerless melt. All the samples were stored in vacuum desiccator until use to avoid moisture contamination.

A part of the melt was cast to produce a glass for the purpose of analysis and characterization. X-ray diffraction analysis (XRD) and examination via scanning electron microscopy (SEM) showed no evidence of unmelted or crystalline particles in the as-quenched glass. The intensity (number of counts per second) of the SiO_2 peak as measured by energy dispersive X-ray analysis (EDS) on 10–12 randomly chosen separate locations, each having the area of ~100 μm × ~100 μm, on the surface of a glass sample was, within experimental error, very close to each other, which suggests for an excellent homogeneity of the as-made glass. No other impurities, including Pt in the 0.001 wt% Pt doped glass, was detected by EDS. The differential thermal analysis (DTA) profile for both the undoped and doped (0.001 wt% Pt) LS_2 glasses was also identical to those reported earlier for similar glasses.

The chemical composition for the as-made glasses was not measured. The primary purpose in the present work was to compare the results obtained from containerless experiments with those from experiments conducted in a container. Since, the glass prepared from the same batch melting was used in both containerless and in-container experiments, any minor change in the chemical composition of the as-made glass from the batch composition should not affect or change the primary conclusions of the present work.

Processing in ESL

The levitation of a specimen in ESL is accomplished by countering the weight (down ward) of the specimen by an upward electrostatic force generated by the electric charge on an electrode and the induced charge on the specimen [12]. In the ESL system at MSFC, three sets of electrodes position the specimen during processing, and comprise the heart of the system. Two dual-axis position sensitive detectors (PSD) in perpendicular direction provide input for the PID control-loop computer, and a stable sample position is maintained by adjusting the control signals provided as in put to the DC amplifiers connected to the electrodes. A detailed algorithm used in the control loop can be found in ref. 10. A 50W CO_2 laser operating at 10.6 μm permits sample heating independent of positioning, and the levitation experiments are typically performed at a pressure of approximately 10^{-10} bar (10^{-5} Pa). A schematic of the MSFC-ESL system, the electrode assembly, and additional technical information can be found at the website http://esl.msfc.nasa.gov

Prior to the experiments in ESL, each spherical glass sample was carefully weighed to an accuracy of ± 0.001 mg, and assigned an identification number for future reference. After levitating, the sample was heated to about 1200 °C (liquidus temperature for this LS_2 glass is 1033 °C) using a controlled heating rate. Controlling the power to the laser source controls the heating and cooling rates of the sample. A maximum heating or cooling rate of 250 °C/s can be achieved by turning the power of the laser source instantaneously on (to the full desired value) or completely off. The spot size of the laser beam was a little larger than the sample size (3–5 mm diameter) so that the beam covered the entire sample. The temperature of the sample was measured by an Impac^{TM} optical pyrometer having a wavelength range 1.45–1.8 μm.

The sample was observed, during processing, using a charged coupled device camera attached to a long-range microscopic lens. A conventional lamp using appropriate heat filters to reduce background noise into the pyrometer illuminated the magnified view of the sample. Images were recorded in standard VHS format for later analysis. A typical temperature-time heating curve for a levitated LS_2 glass when heated at 50 °C/min in the ESL is shown in Fig. 1. The exothermic and endothermic peaks (Fig. 1) correspond to crystallization and melting of the sample, respectively.

A rapid heating of the glass sample produced unwanted disturbance (vibration, oscillation, spinning), causing, in most instances, the sample to be lost from its stable position of levitation. The sample either fell down or moved upwards to stick to the upper electrode. A huge difference in expansion during rapid heating between the glass and the residual gas bubbles in the glass, which were most likely introduced into the glass during fabrication, is suspected to be the reason for the disturbance. As expected, this disturbance in the sample position became more severe during melting when the gas bubbles in the molten sample moved very fast to the top and started bursting randomly from the top surface.

A slow heating rate of 3–5 °C/min was found to be satisfactory to maintain stable levitation of the sample. At this slow heating rate, the gas bubbles in the molten sample were observed to move upwards sufficiently slowly (about 1.5 mm/min) and were removed from the surface one at a time, thus, causing no adverse effect on positional stability of the sample. The sample was kept at 1200 °C until all the gas bubbles were removed, which depended upon the number of gas bubbles the sample contained, but

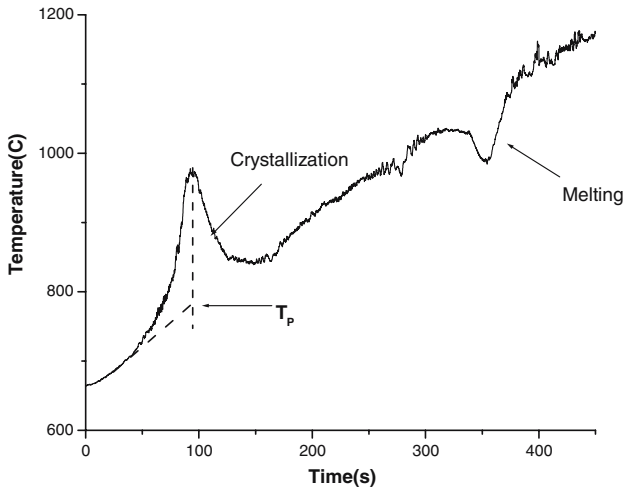

Fig. 1 Typical temperature–time heating curve (at 50 °C/min) for a $Li_2O \cdot 2SiO_2$ glass while levitated at the ESL (MSFC). The exothermic and endothermic peaks correspond to crystallization and melting, respectively, of the glass. Sample diameter: 2.7 mm; sample mass: 24 mg

typically took about 2–3 min. This slow heating schedule was given to all samples that were levitated and processed in the ESL for the first time. Once a sample was made completely free from gas bubbles and solidified to glass, a re-heating at a much faster rate would not seriously affect the stability of the sample for levitation, for example, see Fig. 1 where the sample was re-heated at 50 °C/min after making it bubble-free using a slow heating rate.

After melting at 1200 °C for about 3min, the molten sample was cooled at different predetermined rates to about 300 °C, and a temperature versus time cooling curve was continuously recorded. Any crystallization of the sample during continuous cooling was clearly visible in the real time video image and also by an exothermic change in the cooling curve, Fig. 2. It is to be noted that the same sample can be used in repeated heating-cooling cycles if it is not lost from levitation for any reason. The temperature, T_c, at which the melt crystallized when cooled at a rate, R, was determined from the temperature–time cooling curve, such as one shown in Fig. 2, and the critical cooling rate for glass formation, R_c, was calculated using the following analysis.

The cooling rate, R, at which a crystallization peak is just detectable, was taken as a measure for R_c. Melts that cooled from the melting temperature, T_m, with a rate slower than R_c would crystallize and produce an exothermic crystallization peak in the time–temperature cooling curve. The crystallization temperature, T_c, varies with the cooling rate, R as [30, 31]

$$\ln(R) = \ln(R_c) - \frac{B}{(T_m - T_c)^2} \quad (1)$$

where, B is a constant and T_m is 1033 °C for the LS_2 melt. The critical cooling rate, R_c, for glass formation was determined from the intercept of the plot of $\ln(R)$ versus $1/(T_m - T_c)^2$.

Glasses that were produced by using a rapid quench of the levitated melt at 1200 °C in the ESL, were reheated at different rates, ϕ, and the temperature, T_p, corresponding to the peak of the crystallization exotherm was determined from the temperature-time heating curve, Fig. 1. The effective activation energy for crystallization, E, of the glass was calculated using a Kissinger-type analysis [32], where T_p and ϕ were shown to be related as,

$$\ln\left(\frac{T_p^2}{\phi}\right) = \left(\frac{E}{RT_P}\right) + \text{Constant} \quad (2)$$

where, R is the gas constant. A plot of $\ln(T_p^2/\phi)$ versus $1/T_p$ should result in a straight line whose slope yields the value for E [10, 33]. A glass with a higher value of E should have a higher resistance to crystallization, i.e., a better glass.

In the present containerless experiments in ESL for determining E (Eq. 2), the LS_2 glass was heated at different rates from 2 to 100 °C/min after cooling the melt at the same constant cooling rate of ~250 °C/min, which was achieved by turning off the power to the laser. A constant cooling rate for all the melts ensures the same number of quenched-in nuclei in all the glasses that were available for crystallization in the subsequent heating step.

After processing in ESL, the mass of each sample was again measured and compared with the initial mass. A maximum mass loss of about 0.16 wt% was observed for the sample that was processed continuously (without breaking the levitated mode) for the longest time, about 2.5 h. Since the levitation experiments were conducted in vacuum, evaporation from the surface of the melt is believed to be the reason for this mass loss. The first evaporating species should be Li since its vapor pressure (~3×10^2 Torr) at 1200 °C is higher than that of Si (~10^{-5}) Torr, which would then be followed by O to maintain the oxygen stoichiometry in the melt. However, the small amount of mass loss (0.16 wt%) observed in the present experiments would hardly affect the overall composition of the glass, and, hence, the results of the present work.

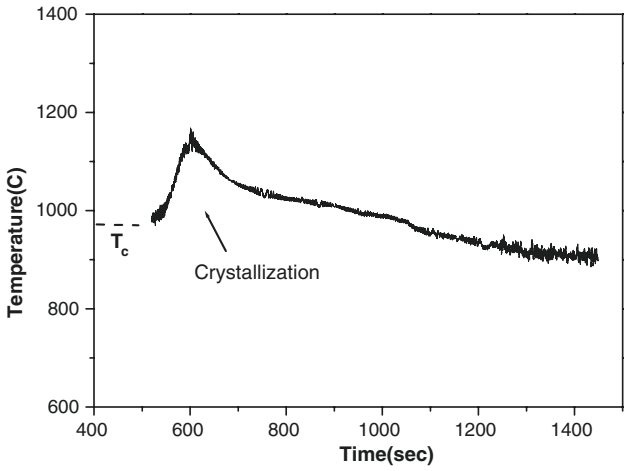

Fig. 2 Typical temperature–time cooling curve at ~11 °C/min for a $Li_2O \cdot 2SiO_2$ melt while levitated at the ESL (MSFC). The exothermic peak corresponds to the crystallization of the melt. The numbers on the horizontal time-axis reflect the elapsed time since the experiment was initially started. For calculating the cooling rate, R (Eq. 1), the time at which the melt temperature reached about 1035 °C (= T_m) was taken as the starting time (zero) for cooling. Sample diameter: 2.5 mm, sample mass: 19 mg

Differential Thermal Analysis (DTA)—experiment in a container

Several spherical glass samples, about 3 mm in diameter, were re-melted at 1200 °C while levitated in ESL for sufficient time to make the melt free from gas bubbles (about 3 min) and cooled at the highest rate achievable by turning the power to the laser source off. These glass samples were then used in DTA (Perkin-Elmer, DTA-7) to measure R_c and E, where the melt or glass remained in contact with a container (DTA crucible). The values of R_c and E measured under container-contact condition in DTA were compared with the R_c and E-values measured under containerless condition in ESL in order to determine whether containerless processing enhances the glass formation tendency for this LS_2 melt. Pre-processing a glass in ESL was not necessary for measuring R_c or E by DTA. Nevertheless, samples processed in ESL were used for the DTA experiments so as to make sure that, like the glass used in the ESL experiments, the glass used in the DTA experiments also did not contain any gas bubble.

The experimental protocol for DTA experiments was generally the same as that used for the experiments in ESL. A spherical glass sample that was pre-processed in ESL was re-melted in a platinum crucible at 1200 °C in DTA for about 3 min, after which the melt was cooled at different pre-determined rates. The values of T_c at different R was determined from the DTA cooling curves, which were then used in Eq. 1 to determine the critical cooling rate for glass formation, R_c.

To determine E, a pre-processed glass sample in ESL was heated in DTA at different heating rates until the crystallization was complete as exhibited by an exothermic peak in the DTA. The values of T_p at different ϕ was determined from the DTA heating curve, and these values were used in Eq. 2 to determine the effective activation energy for crystallization, E.

Due to limited time allotted for these containerless experiments at ESL, only un-doped LS_2 glass samples were prepared for conducting DTA experiments to measure R_c and E, and no DTA experiments for the Pt-doped LS_2 glass processed at ESL were performed.

Results and discussion

It has been possible to successfully levitate, melt (at 1200 °C), and cool spherical LS_2 glass samples, about 3 mm in diameter, in the ESL apparatus. It has been demonstrated also that a molten LS_2 sample can be levitated for any desired length of time, and the same sample can be reprocessed through many different heating-cooling cycles without removing from the ESL apparatus and without breaking the levitated mode. A typical snap shot of a LS_2 glass while levitated at ESL is shown in Fig. 3, which was taken when the glass, after melting and cooling, was reheated at a rate of about 10 °C/min (a), and while the molten glass was held at 1200 °C (b). The picture in Fig. 3(a) corresponds to a time when the temperature of the sample was 665 ± 5 °C, and the sample already started crystallizing, note the bottom opaque part of the sample. Video images showed that the crystals formed initially on the surface of the sample and then moved in wards (in to the bulk) with increasing temperature or time. The glass was kept at 1200 °C until all the bubbles in the glass samples is removed. The circular lines in Fig. 3(b) represent the path of gas bubbles as they move from

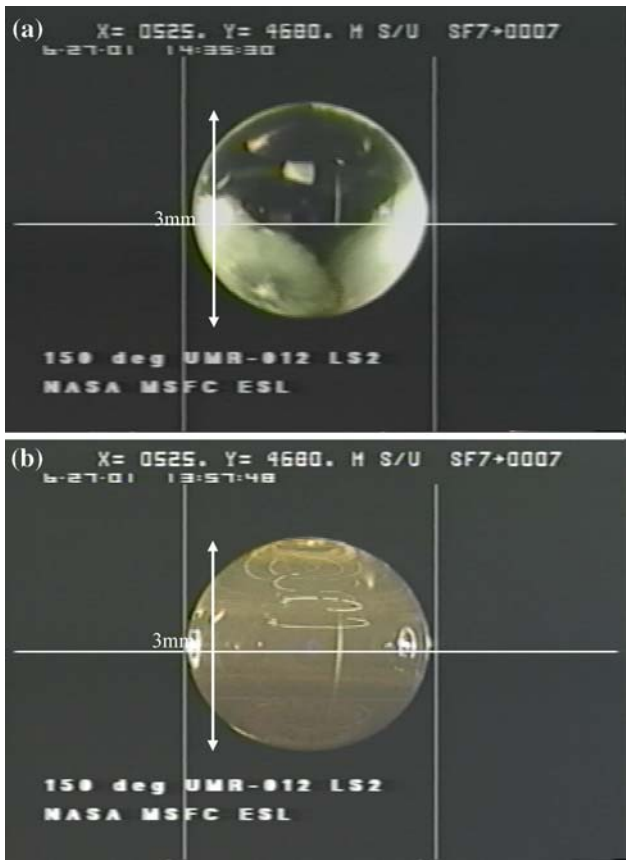

Fig. 3 (**a**) Levitated $Li_2O \cdot 2SiO_2$ glass at ESL when re-heated at 25 °C/min after melting at 1200 °C for 3 min and cooling to room temperature using a fast quench rate (by turning off the power to the laser). This picture corresponds to a time when the temperature was 665 ± 5 °C, and the glass already started crystallizing (lighter areas at the bottom). Sample diameter: 2.5 mm, sample mass: 19 mg. (**b**) The same $Li_2O \cdot 2SiO_2$ glass sample is at molten stage at 1200 °C while levitated at the ESL. The small air bubbles were removed from the top of the sample while levitated. The glass sample was kept at 1200 °C until all the air bubbles were removed

inside to the top of the molten droplet on their way of escaping.

A higher cooling rate (R) depresses the crystallization temperature (T_c) of a melt. As mentioned before, several T_c—values for a melt were determined from the cooling curves obtained at different R. A typical containerless LS_2 melt cooled at about 11 °C/min at ESL is shown in Fig. 2. The onset of the crystallization peak, see Fig. 2, was used as T_c. Figure 4 compares the plots of $\ln(R)$ versus $1/(T_m - T_c)^2$, Eq. 1, for the containerless LS_2 melt (ESL) and for the LS_2 melt in contact with a container (DTA) along with the containerless LS_2 doped with 0.001 wt% Pt glass.

The values for the critical cooling rate for glass formation, R_c, as determined from the intercept of the straight lines in Fig. 4 are given in Table 1, and are about 14 and 62 °C/min for the containerless LS_2 and container-contact LS_2 glasses, respectively. A R_c value of 62 °C/min for the LS_2 glass measured by DTA (container-contact) is in excellent agreement with the similar values reported [34] by others for this glass. The ratio of [R_c(container)/R_c(containerless)] is 4.4, which suggests that the glass formation tendency for a containerless LS_2 melt is increased by a factor of 4–5 compared to an identical melt in contact with a container.

The results also show that the small addition of 0.001 wt% Pt reduces the glass forming ability dramatically. When a glass is doped with a certain number of platinum particles, they form clusters of a size scale comparable to a critical nucleus [7] and act as possible

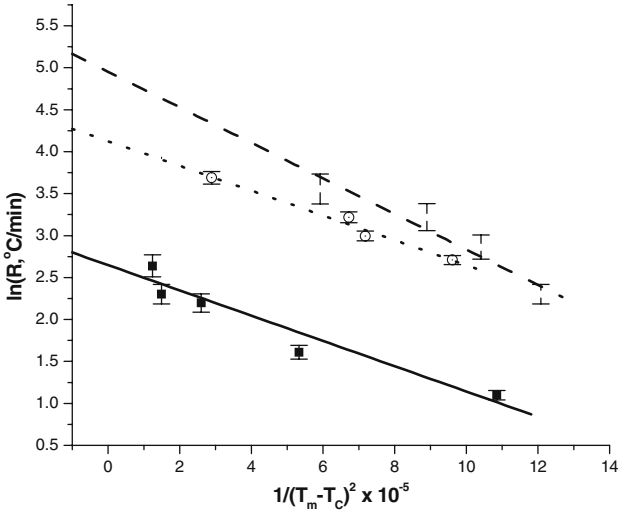

Fig. 4 Plots of $\ln(R)$ versus $1/(T_m - T_c)^2$ (Eq. 1) for the $Li_2O \cdot 2SiO_2$ (LS_2) melts under containerless (ESL) and container-contact (DTA) conditions. (■) LS_2 (containerless, ESL), (▶) LS_2 doped with 0.001 wt% Pt (containerless, ESL), (⊙) LS_2 (container, DTA). Typical sample mass: 20–30 mg

Table 1 Critical cooling rate for glass formation, R_c, and the effective activation energy for crystallization, E, for a $Li_2O \cdot 2SiO_2$ (LS_2) glass as measured by containerless (ESL) and container-contact (DTA) conditions

Glass	Processing condition	R_c (°C/min)	(E ± 15) (kJ/mol)
LS_2	Containerless (ESL)	14 ± 2	392
LS_2	Container (DTA)	62 ± 3	270
LS_2 + 0.001 wt% Pt	Containerless (ESL)	130 ± 5	196

active centers for heterogeneous nucleation. In this work platinum particles were included in order to compare the critical cooling rates for doped and undoped containerless processed LS_2 glass. R_c, as determined from the intercept of the straight lines in Fig. 4 for the containerless LS_2 doped with 0.001 wt% Pt glasses is 130 °C/min. Results indicate that the glass formation for a containerless LS_2 melt reduces by a factor of 9–10 when doped with 0.001%Pt. The R_c data for a container processed LS_2 melt doped with 0.001 wt% platinum is not available, but an unpublished work by one of the present authors (Ray) shows it to be about 170 ± 5 °C/min if such a melt is processed in a container. A smaller R_c, about 130 °C/min, for the Pt-doped containerless melt compred to that (170 °C/min) for an identical melt in a container suggests that containerless processing increases, to some degree, the glass formation tendency of the melt even when it contains some nucleation heterogeneities like Pt. For the two containerless LS_2 melts (ESL), with and without Pt, a higher value of R_c for the melt doped with Pt than that for the melt without Pt clearly shows the expected effect of nucleation heterogeneity on the tendency for glass formation.

The Kissinger plots (Eq. 2) generated using the data from experiments at ESL (containerless) and DTA (container) for the glasses are shown in Fig. 5. Once again, the good linearity of the data points confirms the accuracy of the measurements. The effective activation energies, E, determined from the slope of the straight lines in Fig. 5 are given in Table 1, and are about 392, 270, and 196 kJ/mol for the containerless LS_2 (ESL), container-contact LS_2 (DTA), and containerless LS_2 doped with 0.001 wt% Pt (ESL) glasses, respectively. As mentioned before, a high value of E indicates a high resistance to crystallization or a high tendency to glass formation. The values of E determined in the present work (Table 1) confirms the same general conclusion as that arrived at from the results on R_c, namely, the glass formation tendency for a containerless melt is higher than that for an identical melt in contact with a container.

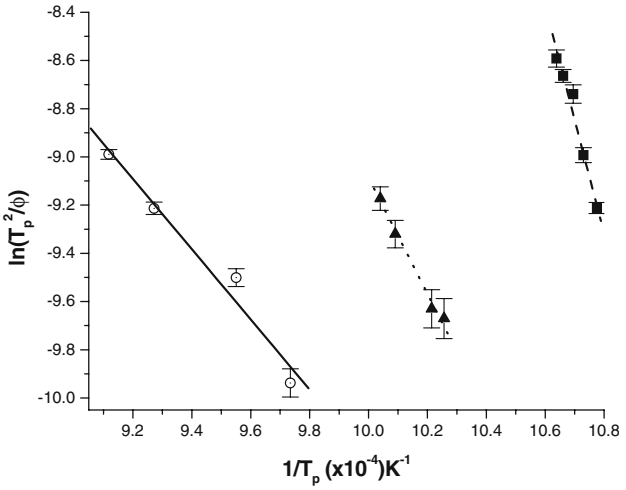

Fig. 5 Kissinger type plots (Eq. 2) for the $Li_2O \cdot 2SiO_2$ (LS_2) glasses under containerless (ESL) and container-contact (DTA) conditions. (■) LS_2 (containerless, ESL), (▲) LS_2 doped with 0.001 wt% Pt (containerless, ESL), (⊙) LS_2 (container, DTA). Typical sample mass: 20–30 mg

Conclusion

Containerless processing of inorganic oxide glass forming melts using the electrostatic levitator (ESL) facility at MSFC has been demonstrated. A stable levitation of the sample for any length of time can be achieved while, simultaneously, the sample is subjected to various heating and cooling cycles between room temperature and 1200 °C. Measurements of the critical cooling rate for glass formation and the effective activation energy for crystallization show that the glass formation tendency for the containerless LS_2 melt increased by a factor of 4–5 compared to an identical melt in contact with a container. The absence of any container-induced heterogeneous nuclei in the containerless melt at ESL is suspected to be the reason for the increased glass formation tendency of this melt.

Acknowledgements This work was supported by the National Aeronautics and Space Administration (NASA), contract # NAG8–1465. The authors thank Trudy Allen and Glenn Fountain for their technical help in processing the samples at MSFC ESL.

References

1. Maurer RD (1959) J Chem Phys 31(2):444
2. Gutzow I (1980) Contemp. Phys 21(3):243
3. Rindone GW (1958) J Non-Cryst Solids 41(1):41
4. Cronin D, Pye LD (1986) Non-Cryst Solids 84:196
5. Lakshmi Narayan K, Kelton KF, Ray CS (1996) J. Non-Cryst Solids 195:148
6. Deubner J, Brukner R (1993) J Non-Cryst Solids 163:1
7. Gutzow I, Schmelzer J (1995) The vitreous state: thermodynamics, structure, rheology, and crystallization. Springer, Berlin, p 217
8. Uhlmann DR, Yinnon H (1983) In: Uhlmann DR, Kreidl NJ (eds) Glass science and technology, vol 1. Glass forming systems. Academic Press, New York, NY, chapter 1
9. Scherer GW (1991) In: Cahn RW, Haasen P, Kramer EJ (eds) Materials science and technology, vol 9. Glass and amorphous materials. VCH Publications, New York, NY, chapter 3
10. Ray CS, Day DE (1984) J Am Ceram Soc 67:806
11. Rogers JR, Hyers RW, Rathz T, Savage L, Robinson MB (2001) In: El-Genk MS (ed) Proceedings of the space technology and applications international forum 2001, Albuquerque, Nm, AIP Conf. Proc., vol 552, p 332
12. Rogers JR, Robinson MB, Hyers RW, Savage L, Rathz T (2000) In: Robert A. Schiffman (ed) 12th international proceedings of the experimental methods for microgravity materials science, ASM International
13. Rhim WK, Chung SK, Barber D, Man KF, Gutt G, Rulison AJ, Spjut RE (1993) Rev Sci Instrum 64:2961
14. Rulison AJ, Watkins JL, Zambrano B (1997) Rev Sci Instrum 68:2856
15. Hays CC, Schroers J, Johnson WL, Rathz TJ, Hyers RW, Rogers JR, Robinson MB (2001) Appl Phys Lett 79:1605
16. Kelton KF, Lee GW, Gangopadhayay AK, Hyers RW, Rathz TJ, Rogers JR, Robinson MB, Robinson DS (2003) Phys Rev Lett 90:195
17. Yu J, Koshikawa N, Arai Y, Yoda S, Saitou H (2001) J Cryst Growth 231:568
18. Paradis PF, Ishikawa T, Yu J, Yoda S (2002) Proceedings of 40th AIAA aerospace sciences meeting and exhibit, Reno, Nv, USA, 14–17 January 2002
19. Zanotto ED, James PF (1990) J Non-Cryst Solids 124:344
20. Potpov OV, Fokin VM, Filipovich VN, Kalinina AM (1998) Glass Phys Chem 24(4):337
21. James PF, Scott B, Armstrong P (1978) Phys Chem Glasses 19(2):24
22. Fokin VM, Potpov OV, Chinaglia CR, Zanotto ED (1999) ibid. 258:180
23. Strand Z, Douglas RW (1973) Phys Chem Glass 14(2):33
24. Gonzalez-Oliver JR, Johnson PS, James PF (1979) J Mater Sci 14:1159
25. Ray CS, Fang X, Day DE (2000) J Am Ceram Soc 83:865
26. Barta C, Stourac L, Triska A, Kocka J, Zavetova M (1980) J Non-Cryst Solids 35:1239
27. Ray CS, Day DE (1987) In: Doremus RH, Nordine PC (eds) Mat. Res. Symp. Proc., vol 87, p 239
28. Frischat GH (1995) J Non-Cryst Solids 183:92
29. Ray CS, Day DE (2003) J Thermophys Heat Transfer 17:174
30. Barandiaran JM, Colmenro J (1981) J Non-Cryst Solids 46:277
31. Huang W, Ray CS, Day DE (1986) J. Non-Cryst Solids 86:204
32. Kissinger HE (1956) J Res Natl Bur Stand (US) 57:217
33. Ray CS, Huang W, Day DE (1991) Am Ceram Soc 74:60
34. Bansal NP, Doremus RH (1986) In: Handbook of glass properties. Academic Press, New York, NY